Table of Contents

List of Tables and Figures

I. INTRODUCTION

This investigation was sponsored by the David Taylor Research Center (DTRC) under contract to the Department of Naval Architecture and Marine Engineering, Program in Ship Hydrodynamics (PSH), College of Engineering, The University of Michigan. The purpose of this investigation was two fold. First, to provide Lagrangian velocity profiles in the near wake region of a high speed twin screw vessel and second, to apply advanced spatial domain stochastic analysis techniques to radar images of surface ship wakes obtained during the Spaceboard Imaging Radar-B (SIR-B) Shuttle mission. These two activities are related through a desire to obtain greater knowledge of the complex hydrodynamics in operation in the viscous wake region of modern surface ships and how these interactions affect active remote sensing of the ocean surface. Discussion of the SIR-B portion of this investigation is provided as a separate document.

The purpose of this investigation was to provide surface Lagrangian velocity profiles in the viscous wake region utilizing the Digital Automated Radar Tracking System (DARTS). Two-dimensional viscous wake velocity profiles were desired from the stern of the vessel to as many ship length aft as was feasible within the constraints and limitations of the test basin. The "downstream" rate of decay of both the transverse and longitudinal velocity components were of primary interest for numerical model verification. The final goal of this investigation was to provide an experimental foundation upon which to guide full-scale measurement efforts.

The Lagrangian velocity analysis utilized hardware and software developed in conjunction with the Digital Automated Radar Tracking System (DARTS) to acquire trajectories of tag particles seeded in the near wake region of a towed twin screwed high speed vessel model. For this application, the radar portion of the DARTS system was replaced by a conventional high resolution video camera system. Video images were digitized and examined for each particle location and velocity with successive data runs compiled in a statistical framework. As a result of this investigation, nearly 30,000 velocity observations were obtained in the viscous wake region from immediately astern of the transom to approximately five ship lengths down stream. Although towed in the Ship Hydrodynamics Laboratory (SHL), the vessel propeller loading was adjusted to simulate a self-propelled vessel. Due to limitations of time

and money, only the twin screwed, outboard rotation data runs have been analyzed in detail and compiled in this summary, although wake fraction survey coverage exists for single screw as well as no propeller operation cases.

II. SHIP HYDRODYNAMIC TEST FACILITY

The University of Michigan Ship Hydrodynamic Test Facility (Tow Tank) was the site for the model scale experiment described herein. The Tow Tank is the largest University owned model testing facility in the United States. It is 360 feet (109.7 m) long, 22 feet (6.7 m) wide and 10 feet (3.05 m) deep. Mounted on rails over the tank is the main carriage and subcarriage which serve to transport data acquisition and analysis devices, ship models and personnel at speeds from 0.25 ft/s (0.0760 m/s) to 20.0 ft/s (6.0840 m/s) at an accuracy of 0.02 ft/s (0.0061 m/s).

1. Experimental Configuration

This project was a continuation of work done in 1987 under University of Michigan project number 023945. Refinement was made in the test technique and additional data acquired. A schematic representation of the test apparatus is provided in Figure 1.

The purpose of this test was to optically track targets dropped at known locations in the surface wake. The drop device was the same one used in the 1987 tests. This dropper places fifteen targets (referred to as DARTS) at two inch intervals normal to the direction of model travel. Longitudinal as well as transverse offset of the DART dropper were utilized to acquire complete coverage of the wake region of interest. (see Figure 2). The targets used were luminous polyethylene 0.25 inches (63 mm) in diameter and 0.06 inches (15 mm) thick and were slightly buoyant to provide a true representation of the surface velocity.

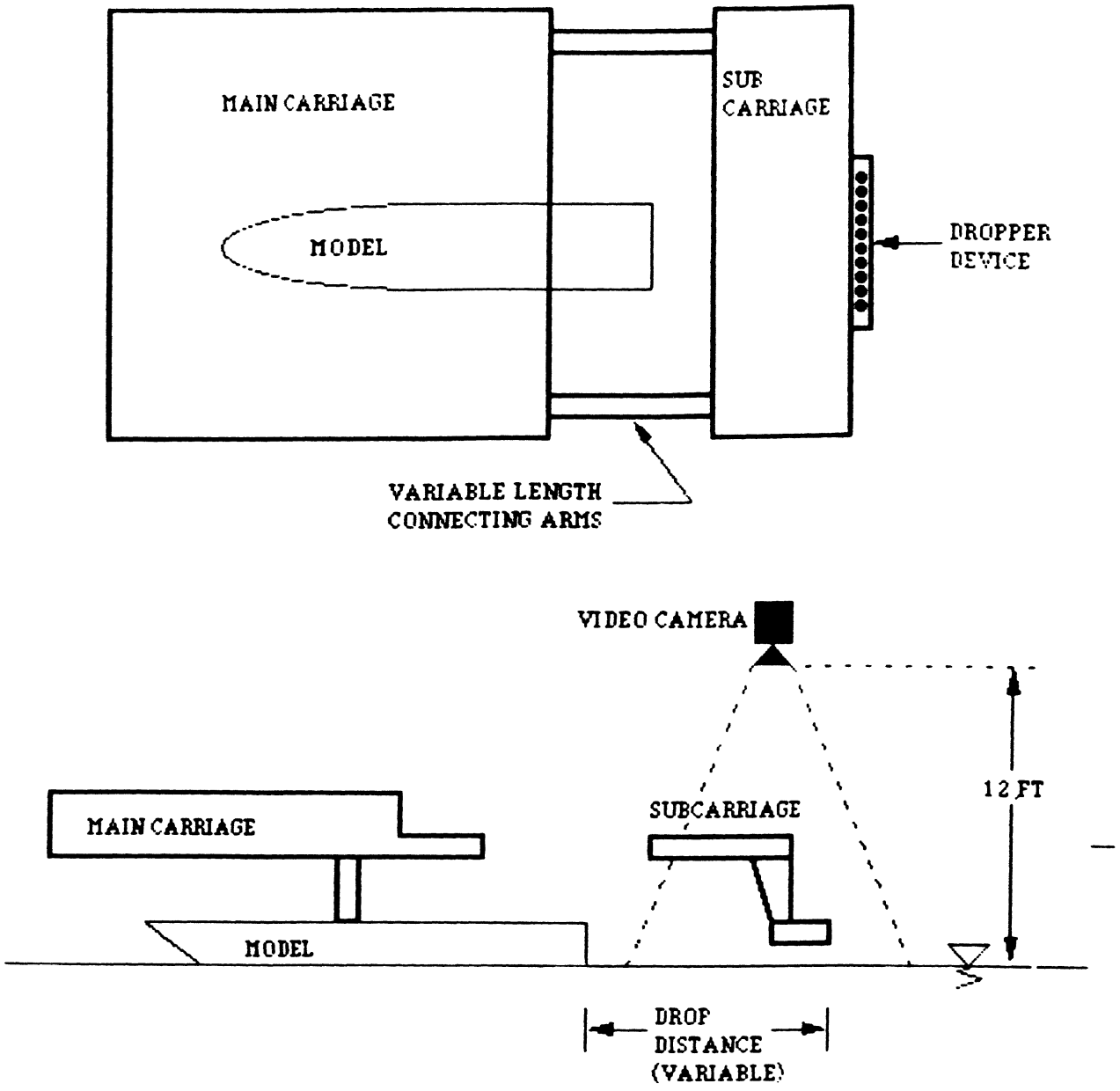

Figure 1. Schematic representation of test apparatus.

The model used for these tests (DTRC No. 5369-1) was provided by the sponsor and was numbered U of M 1597 for internal bookkeeping purposes. This was the same model tested in 1987 as U of M 1581 and is a 1:24.824 scale model of high speed twin screw vessel with a model length of 24.84 feet (7.57 m) and a beam 2.204 feet (0.67 m). The narrow beam of this ship necessitated the placement of the starboard engine room aft of the port engine room. This geometry resulted in a shallower inclination angle of the port propeller shaft. The model appropriately displays this cross-ship assymetry. The propellers used in the test were also provided by DTRC and were operated with outboard rotation.

Figure 2. Wake coverage showing longitudinal and transverse offsets.

The test section of the model basin was darkened and illumination of the targets was provided by an array of ultra violet fluorescent lights. A Pulnex model TM-540 high resolution nadir viewing video camera was mounted approximately twelve feet above the water surface on the dropper centerline. The video signal was recorded simultaneously in the U-Matic format on a Sony VO-5600 and in VHS format on a General Electric 9-7885. The U-Matic tapes were saved as an archival record while the VHS tapes were used for the actual data reduction.

2. The Model Tests

This test series was run at the design displacement for one speed (20 knots (10.3 m/s) full-scale) in the normal, no propeller, and trail shaft propulsion modes. Propeller rotation was outboard and model rpm settings were determined from full scale trial data from the same class ship. All trail shaft tests were performed with the starboard shaft trailing. Two runs were made without any propellers mounted to compare with the 1987 data.

Data runs were taken with the DART dropper on centerline and one-half model beam to port and starboard at six distances aft for both standard and trail shaft conditions. Figure 2 provides a schematic representation of the region of wave coverage. Each configuration was run a minimum of five times to indicate level of repeatability. Table I provides a summary of the test matrix. A "zero drift" was taken for one minute before each series of runs (one per camera location) to verify still water conditions in the tow tank facility using 1.0 inch (254 mm) diameter 0.06 inch (15 mm)

thick yellow balsa targets. For the zero drift runs the targets were scattered randomly within the field of view and video taped under fluorescent light.

Individual data runs were recorded for varying lengths of time depending on the length of time it took for the targets to migrate out of the field of view. No runs were longer than sixty seconds and twenty to thirty seconds was typical.

Table I. Test Matrix Summary

	Normal Propulsion						Trailing Shaft						No
Aft Dist (L)	0.00	0.07	0.21	0.50	1.00	1.60	0.00	0.07	0.21	0.50	1.00	1.60	1.60
Centerline	8	10	5	9	6	5	5	5	8	8	5	5	2
14" Port	5	5	5	5	5	9	5	6	5	5	5	9	
14" Stbd	5	5	5	6	5	5	5	6	5	5	5	6	
Totals	18	20	15	20	16	19	15	17	18	18	15	20	2

Although most data runs went smoothly, a few problems were experienced early in the test sequence. The most serious problem was the loss of the starboard propeller shaft during run 10. Repairs were made and the tests continued without mishap until run 29, when the drop distance was set at 0.07 lengths aft of the model. At this point the stern wave crest was high enough to wash the darts off the dropper. Since the dropper was fixed in vertical position, the solution was to lower the water level in the model basin two inches, refocus the camera, and take a new calibration grid measurement. There were minor problems experienced in obtaining a perfect match between desired and the actual propeller rpm. In general, the variations were small; ± 1 rpm in model scale. The actual rpm was recorded for each run. A complete list of all data runs is given in Appendix A.

III. LaGRANGIAN TRAJECTORY ANALYSIS

1. Data Reduction

The dart trajectories for each run were recorded on color video tape with a black and white, high resolution, low light camera using 625 horizontal lines per screen and 1/30 second between frames. A digital timer was displayed on the screen to give the elapsed time after the passage of the stern of the model for each frame. An Imaging Technology frame grabber board was used with a DEC Microvax GPX workstation to freeze every third frame and extract the X-Y position of the center of each visible dart in screen pixel dimensions.

After an entire run was digitized, a specialized MacIntosh computer application was used to identify each individual dart trajectory, calculate the velocity components and store this data in standardized format files. For any unrecorded, or unknown positions or velocities, a missing data value was used. The data was then analyzed for quality control and unacceptable velocity measurements, due to digitizing error, were set to the missing data value.

All of the data was then transformed into ship co-ordinates, and non-dimensionalized into longitudinal and transverse wake fractions. An Apollo computer application performed the co-ordinate transformation based on conversion factors for pixel size, time counter calibration, ship speed and camera position. The coordinate system is provided in Figure 3. Longitudinal positions (x) indicate ship lengths aft of the model transom. Positive transverse positions (y) indicate ship beams starboard of

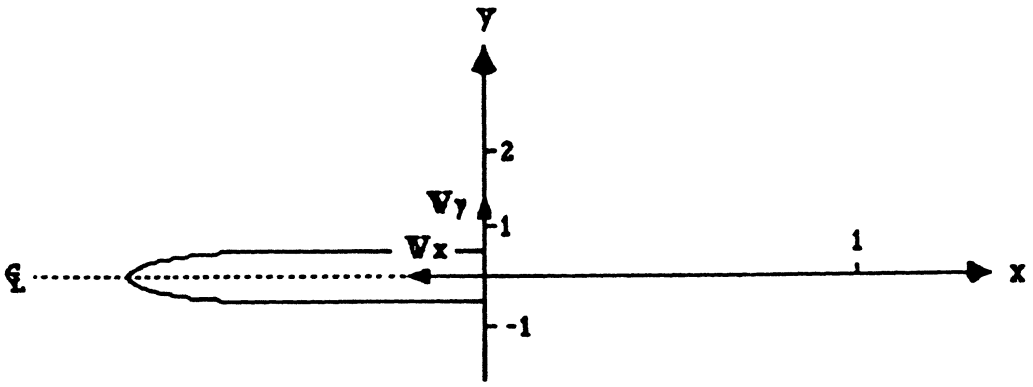

Figure 3. Coordinate system for analysis results.

the model centerline. Velocities indicate fraction of the model speed in the direction of ship motion (Wx) and to starboard (Wy).

The approximate size of the region where the darts fell in ship coordinates was 120 by 9 feet (36.58 by 2.74 m) in the X and Y directions, respectively. For analysis, this region was divided into 120 one-foot long (0.304 m) and 19 one-half-foot (0.152 m) wide bins, for a total of 2507 bins. This was the most convenient bin size selection as it gave excellent resolution with the minimum number of total bins and even values of distances for graphical display. A further discussion of the sensitivity of the analysis to bin size selection is provided in the next section. The target position data was then apportioned to the nearest bin. Figure 4 graphically shows the number of darts found in each bin for all runs combined. It should be noted that the distribution of velocity measurements covers the entire central position of the chart up to 98 feet (29.87 m) aft.

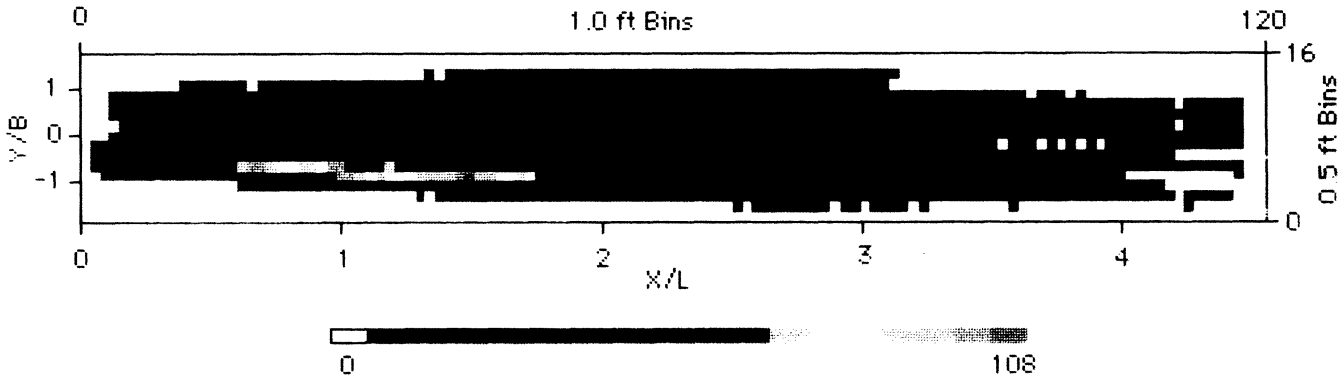

Figure 4. Velocity measurement point density by bin location.

2. Statisical Analysis and Digital Filtering

The following discussion focusses on the statistical significance of the DARTS data set and the subsequent analysis of digitally filtered velocity matrices. The superposition of the data set is examined as well as the statistical impact of bin size selection, averaging and filtering procedures.

To analyze the statistics for each individual bin, values of sample mean and variance are required. To calculate the variance, at least three data points are required in each bin. Of the 2507 bins in the 120 by 19 grid, 172 (6.8%) had fewer than three points. These were invariably along the edge where the distribution of darts dropped off to zero. Consequently, there were about 2335 bins that could be analyzed statistically. The sample mean and variance of these bins were calculated and then each point in every bin was examined to see what minimum confidence interval was required to have that point included in a normal distribution. Figure 5 shows an example of the probablility density function of one bin. It corresponds to the position 37 feet (11.28 m) behind and 2 feet (0.61 m) to port of the ship origin with 96 data points. A list was generated for points that were more than 3 standard deviations away from the average. It would be expected for a normal distribution that 0.5% of all points would extend outside those limits. One hundred ninety four (194) points (0.66%) were found for W_y and 259 (0.88%) for W_x, out of the 29,535 points recorded. This analysis suggested that leaving all of the points in the data set for analysis would not affect the results.

During a single run at one ship speed, dart dropper location, and camera position; darts were released and tracked in a relatively small area, approximately 2 by 40 feet (0.61 by 12.19 m). Therefore, it was necessary to superimpose data from different dropper locations to fill the 9 by 120 foot (2.74 by 12.19 m) area behind the ship. Initially, this was done by combining all runs for the largest dropper distance (1.6 ship lengths) and sequentially adding closer dropper distance runs (1.60, 1.00, 0.50, 0.21, 0.07, 0.00 ship lengths).

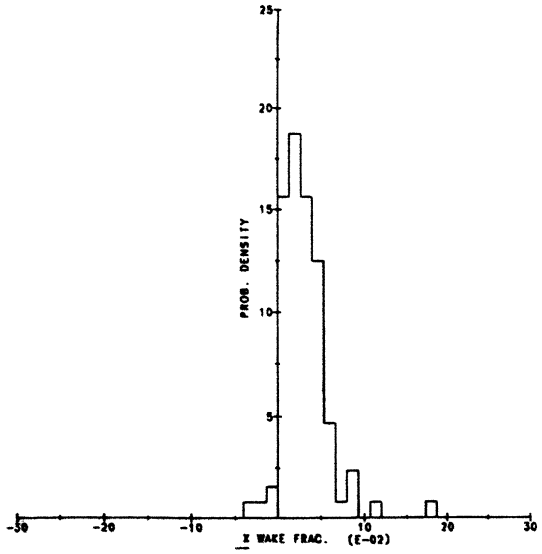

Figure 5. Probability density function for the bin corresponding to 37 feet (11.3 m) aft and 2 feet (0.6 m) port of the ship origin with 96 data points.

Figure 6. Successive superposition of centerline longitudinal wake fraction by dropper distance.
A. 1.60 X/L, B. 1.60-1.00 X/L, C. 1.60-0.50 X/L, D. 1.60-0.21 X/L,
E. 1.60-0.07 X/L.

The results are shown in contour image diagrams, Figures 6A through E for W_x and Figures 7A through E for W_y, both with the camera on centerline. It can be seen that there is a minimum of variation as the additional data is added in sequence, rather, the field becomes increasingly more well defined. This self consistency also held for the port and starboard camera and dropper offset positions, but was not so clearly defined between the center, port and starboard data sets. Consequently, these three large data sets were built and it was assumed that any internal errors were random and small. It is possible that the cross-ship variations of ship structure and propulsion influence the cross-ship data set consistency. For the sake of an overall picture, all three data sets (center, port and starboard) were superimposed and are shown in Figures 8 and 9 as W_x and W_y contour images, respectively. It will be seen later in this discussion that by first filtering the three transverse offset datasets, that they can be superimposed to advantage.

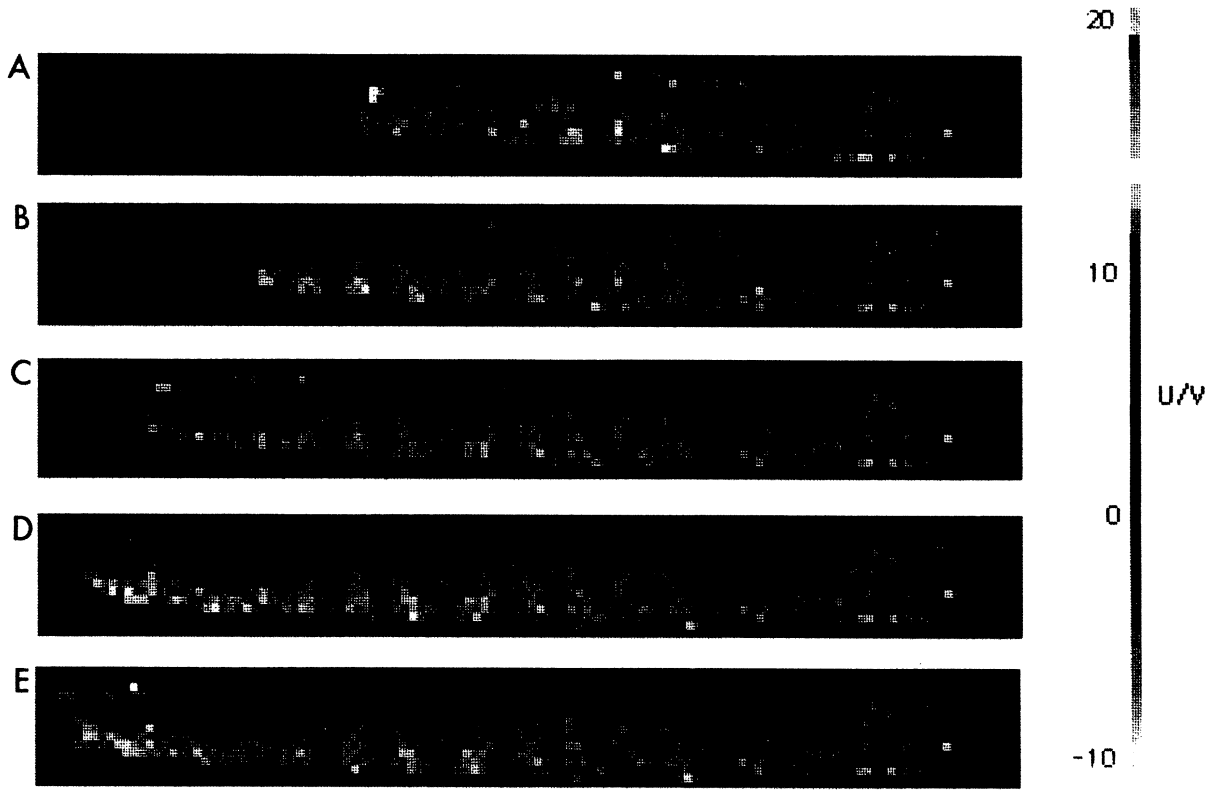

Figure 7. Succesive superposition of centerline transverse wake fraction by dropper distance.
A. 1.60 X/L, B. 1.60-1.00 X/L, C. 1.60-0.50 X/L, D. 1.60-0.21 X/L,
E. 1.60-0.07 X/L.

Figure 8/9. Superpostion of longitudinal/transverse wake fraction, combination of starboard, centerline and port datasets.

This data set could also be displayed along longitudinal and transverse cuts in the ship's flow field. Figures 10 and 11 show this for the unfiltered combined data along longitudinal cuts of -1.5 feet (-.46 m), 0.0 feet and +1.5 feet (0.46 m) from the ship centerline for W_x and W_y. Figures 12 and 13 show transverse cuts at 21.0, 23.0, 25.0 and 27.0 feet (6.40, 7.01, 7.62, and 8.22 m) from the stern for the same unfiltered data group.

The effect of variation in bin size was negligible within the constraints of having enough points in each bin for accurate average values of wake fraction, and having enough bins to show some detail in the spatial wake variation. By reducing the number of bins, there were more points per bin, but still the same approximate proportion (i.e. 5%) of bins that had fewer than three points necessary to calculate statistical quantities. The effect, shown unfiltered in Figure 14 is similar to a crude form

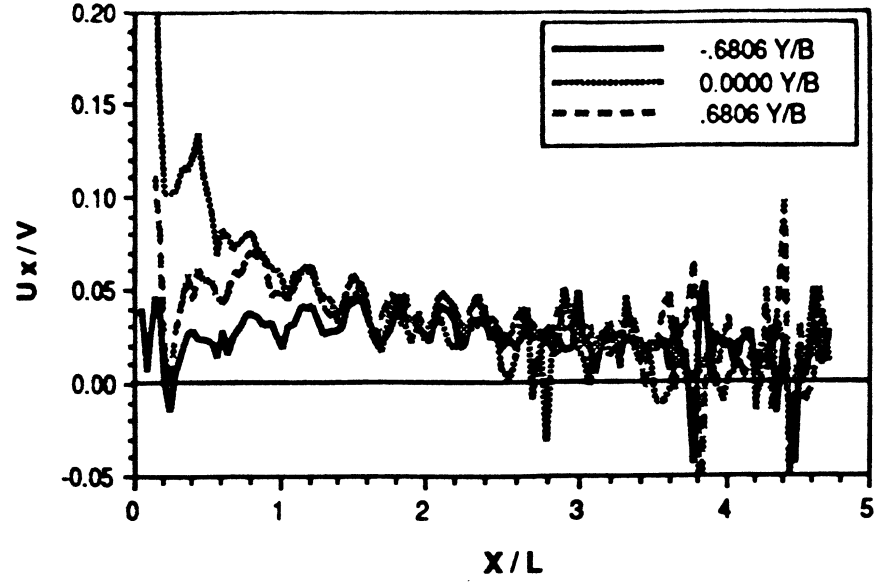

Figure 10. Longitudinal surface wake fractions as a function of distance aft, for longitudinal slices along the port, starboard and centerline of Figure 8.

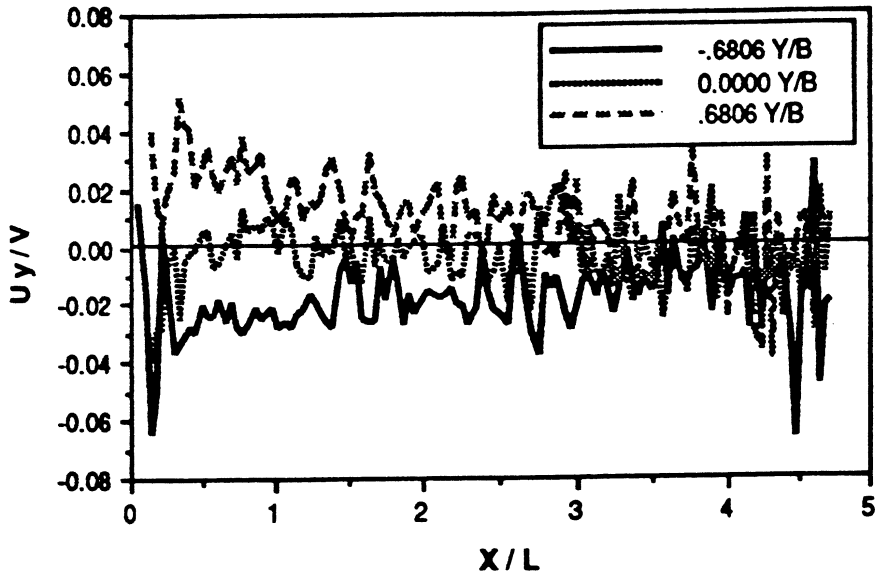

Figure 11. Transverse surface wake fractions as a function of distance aft, for longitudinal slices along the port, starboard and centerline of Figure 9.

of filtering, that is an average across adjacent bins. However, where there are rapid fluctuations, such as beyond 90 feet (27.43 m), the low-pass filtering is better. Note the oscillations in Figure 15 using fewer bins, compared to Figure 17 using the filter. By increasing the number of bins, the frequency response could be increased, but the frequency of interest in water waves is generally low, so that the additional computational effort was not warranted.

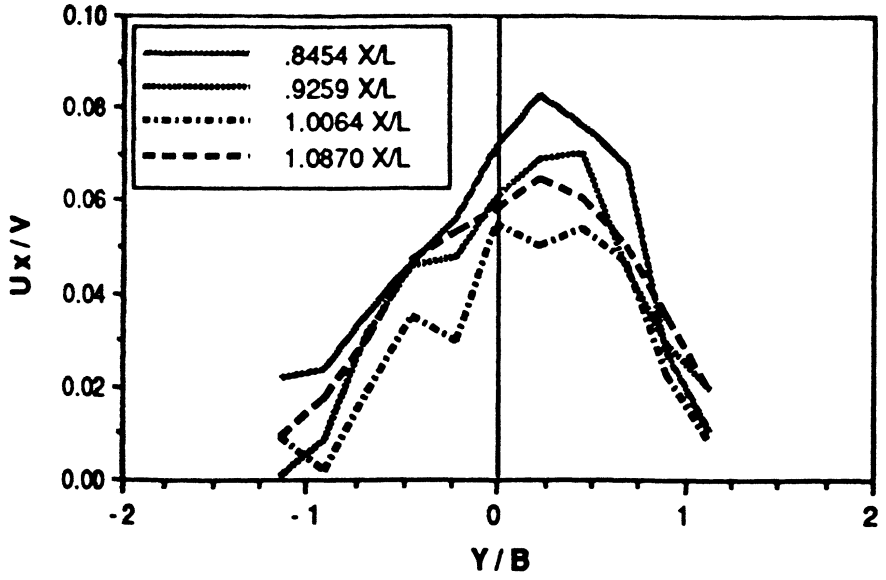

Figure 12. Longitudinal surface wake fractions as a function of distance starboard, for transverse cuts through Figure 8.

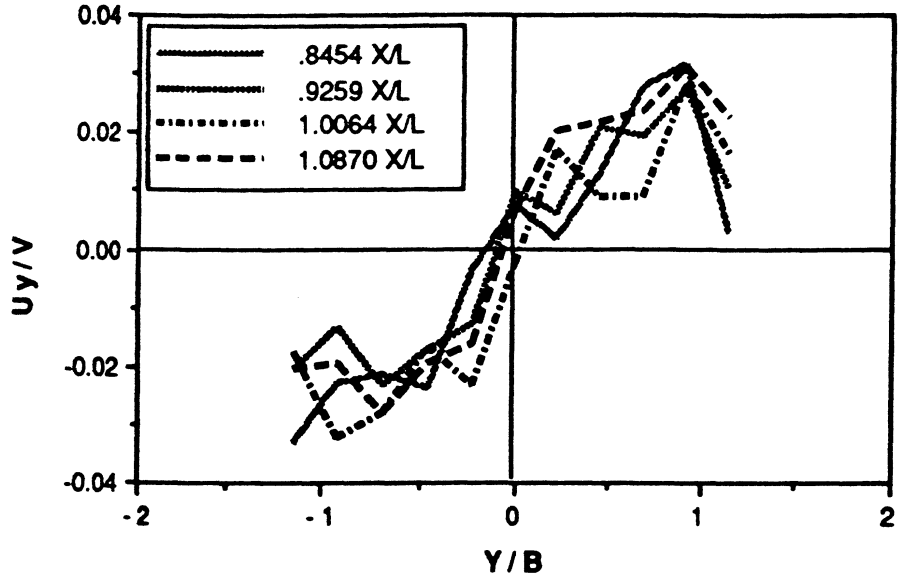

Figure 13. Transverse surface wake fractions as a function of distance starboard, for transverse cuts through Figure 9.

The low-pass filter applied in this analysis is symmetric and non-recursive so there is no phase shift at any frequency. The lag window chosen to filter over depended on the "cutoff wavelength", ω_c. The cutoff is in terms of a wavelength based on the size of the bins, so $\omega_c = 1.0$ means all frequencies that generated waves of less than 1 bin were removed. Recall that the bins are 1 foot (0.304 m) long and one-half

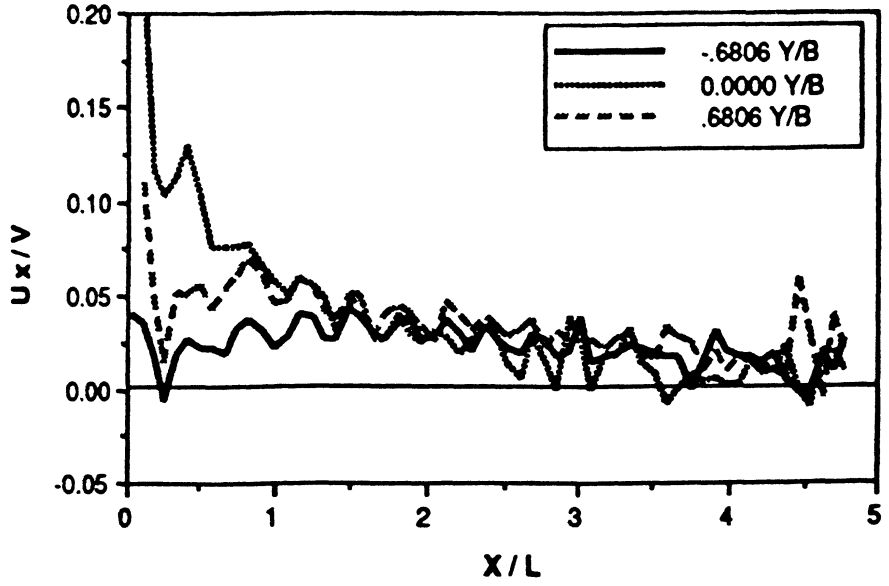

Figure 14. Longitudinal surface wake fractions as a function of distance aft after reducing the number of bins to 61.

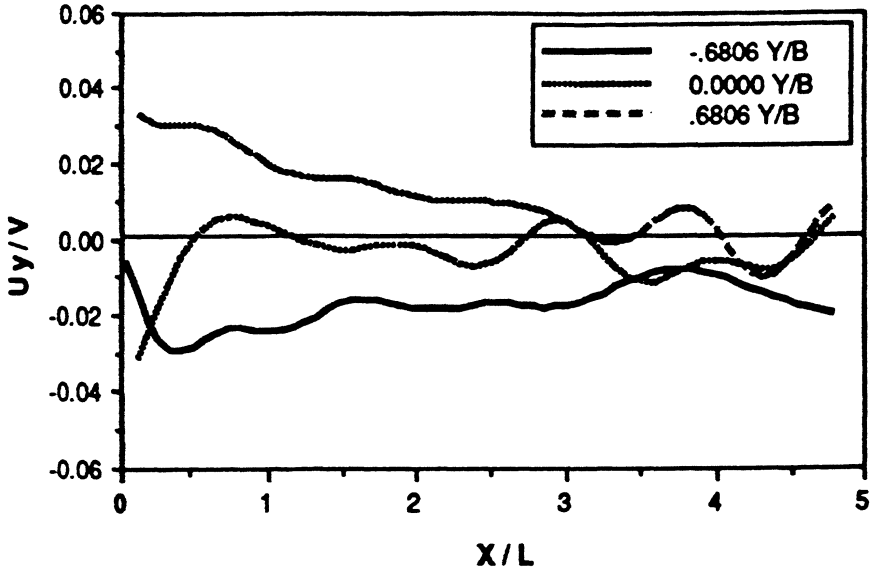

Figure 15. Longitudinal surface wake fractions as a function of distance aft after reducing the number of bins to 61 and filtering.

foot (0.152 m) wide, so the same cutoff value differs in effect in the transverse direction from the longitudinal direction. Thus the lag window was chosen to be just sightly larger than the cutoff wavelength.

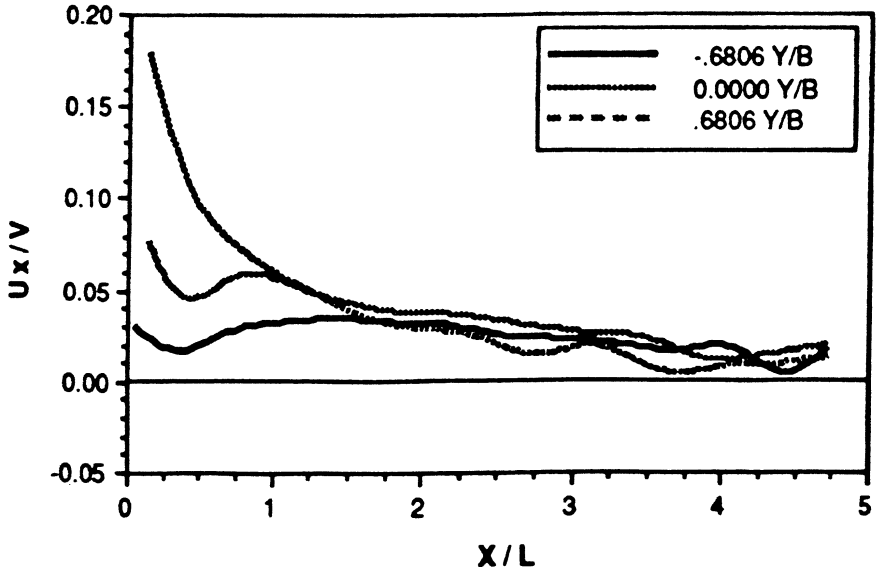

Figure 16. Downstream surface wake fractions as a function of distance starboard, for longitudinal cuts through Figure 10, heavy filtering (ω=0.05, L=25).

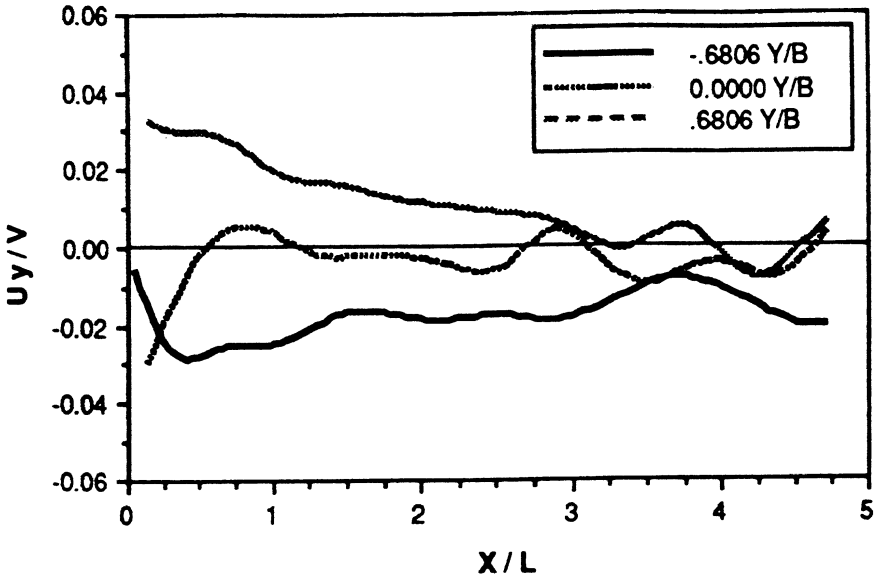

Figure 17. Cross-stream surface wake fractions as a function of distance starboard, for longitudinal cuts through Figure 11, heavy filtering (ω=0.05, L=25).

With a lag window of 25 bins and a very low cut-off frequency of $\omega_c = 0.05$ cycles per bin in the longitudinal direction only, the filter essentially generates the D.C. signal as shown in Figures 16 and 17. The average wake values fall nicely over the unfiltered plots, Figures 12 and 13, showing no distortion due to the extremely heavy filtering.

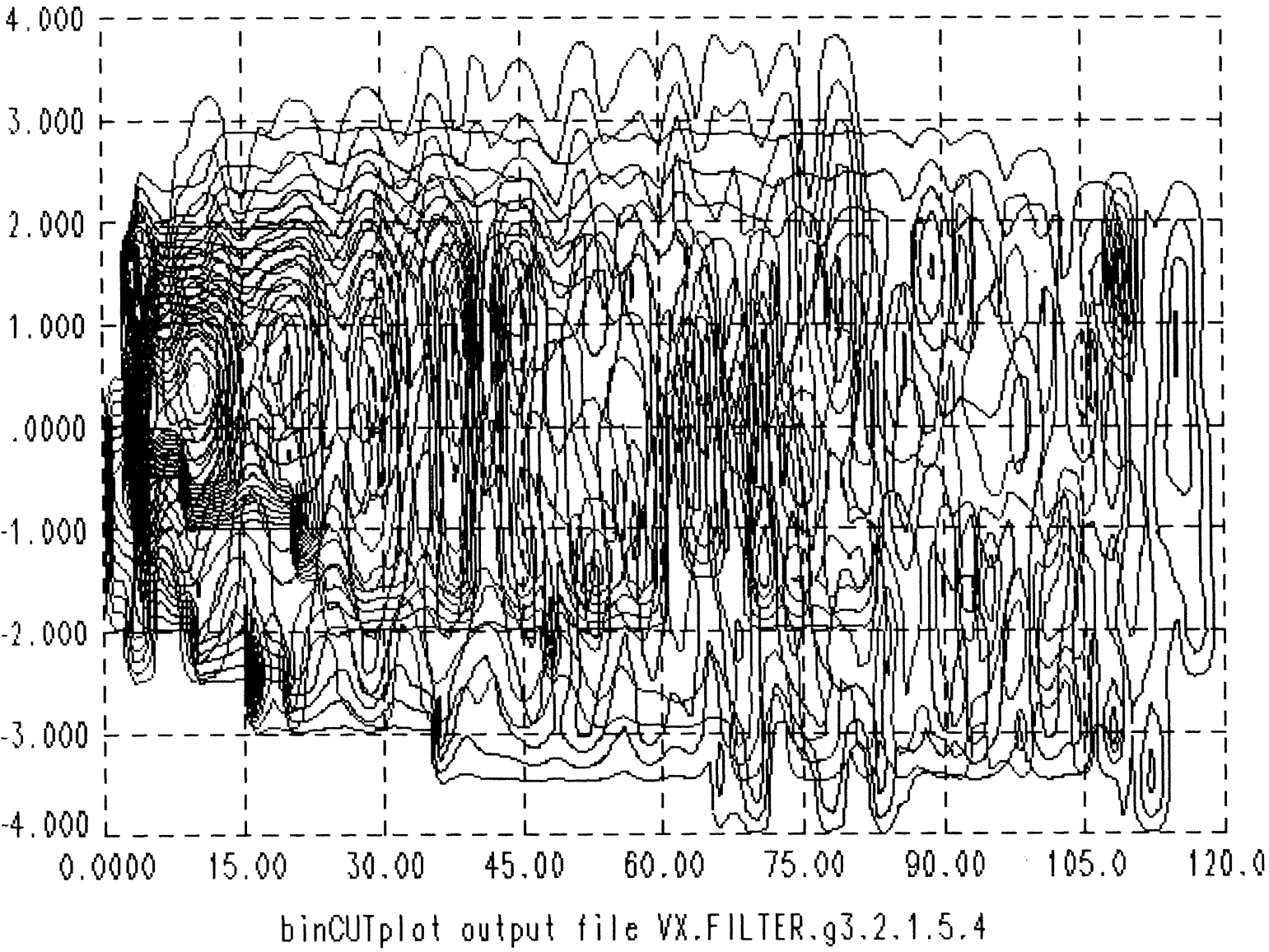

Figure 18. Color contour plots showing Wx superposition after light filtering (ω_x=0.35, L_x=5,ω_y=0.45,L_y=4).

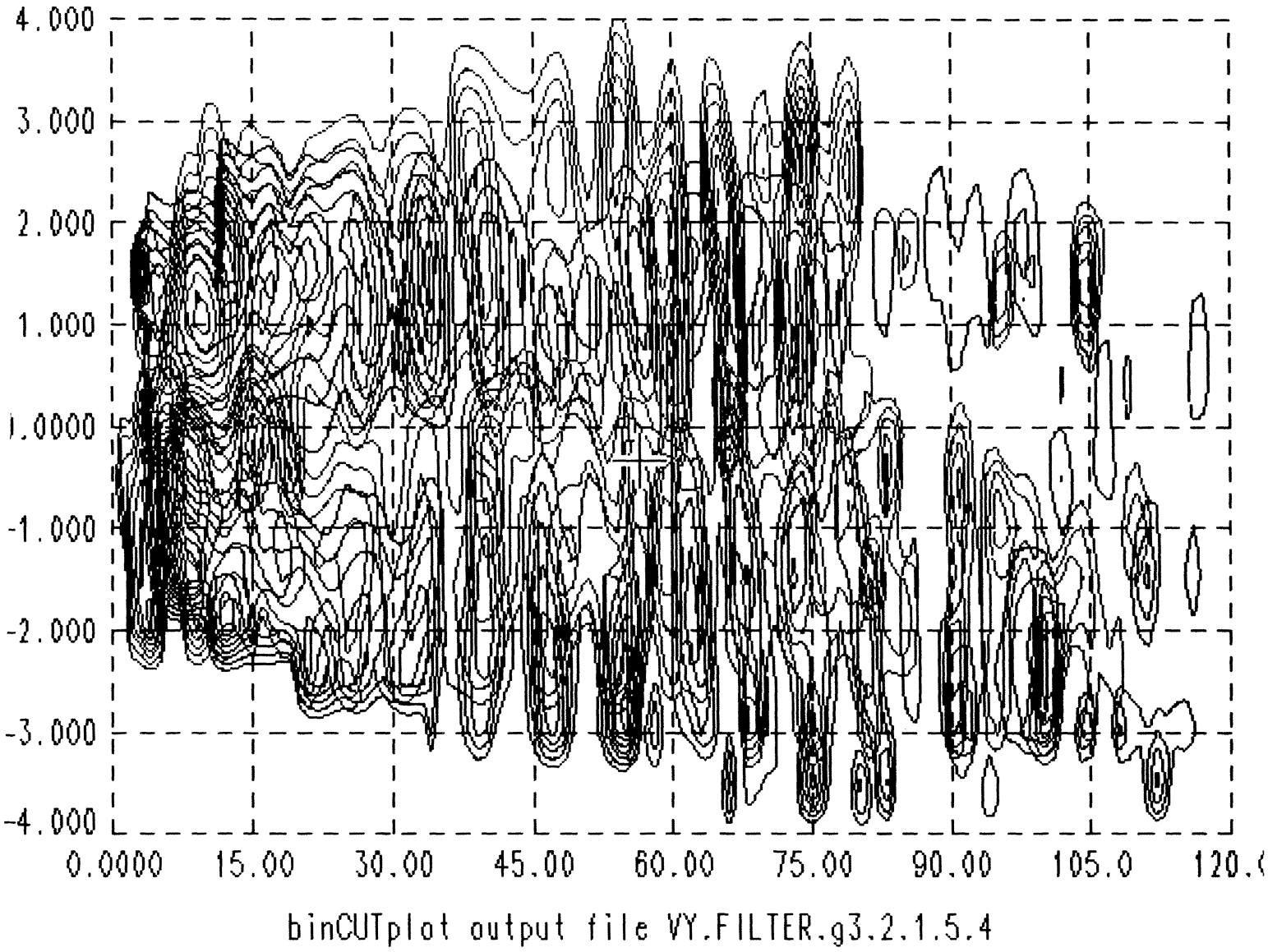

Figure 19. Color contour plots showing Wy superposition after light filtering (ω_x=0.35, L_x=5,ω_y=0.45,L_y=4).

For a lag window of five bins and a higher value of ω_c = 0.35 in the longitudinal direction combined with a lag of four bins and ω_c = 0.45 in the transverse direction, the center, port, and starboard data can be overlaid to advantage. Color plots of W_x and W_y are shown in Figures 18 and 19 for the center, port, and starboard cases. For W_y, only negative values of velocity were plotted for port measurements and only positive values for starboard to reduce unnecessary clutter. For W_x, the values at x = 10, 20, 30, 37 and 45 feet (3.05, 6.10, 9.15, 11.28, and 13.72 m) show the near-field peaks line up extremely well, while for W_y, the far-field peaks at 35 to 75 feet (10.67 to 22.86 m) correspond well. The outermost contour lines do not have much significance as they simply indicate the outer range of the data which, of course, changes with dart dropper location. The resultant matrix of this superposition is shown in Figures 20 and 21. Utilizing this filtering configuration, the longitudinal plane cuts look essentially

Figure 20/21. Resultant contour image of Figure 19 showing Wx/Wy superposition after light filtering (ω_x=0.35, L_x=5,ω_y=0.45,L_y=4).

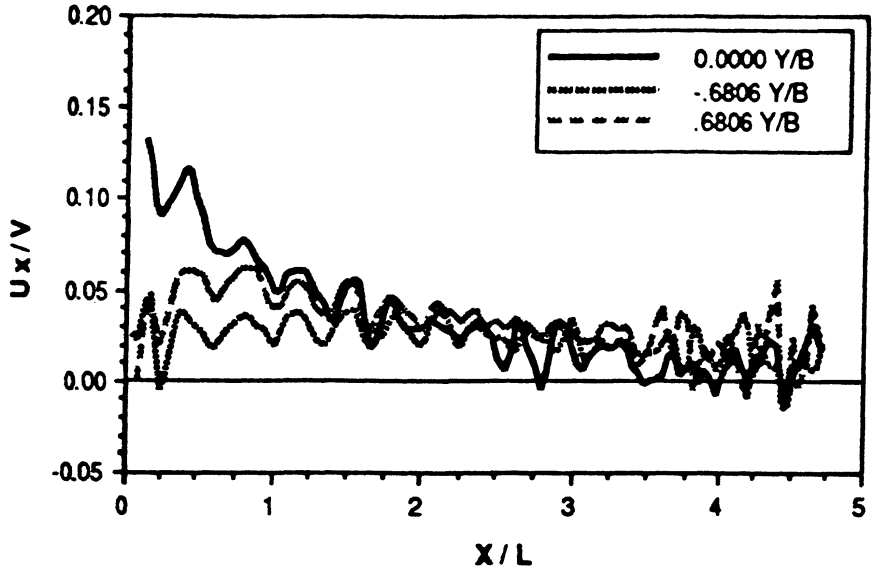

Figure 22. Downstream surface wake fractions as a function of distance starboard, for longitudinal cuts through Figure 20, light filtering (ω_x=0.35, L_x=5,ω_y=0.45,L_y=4).

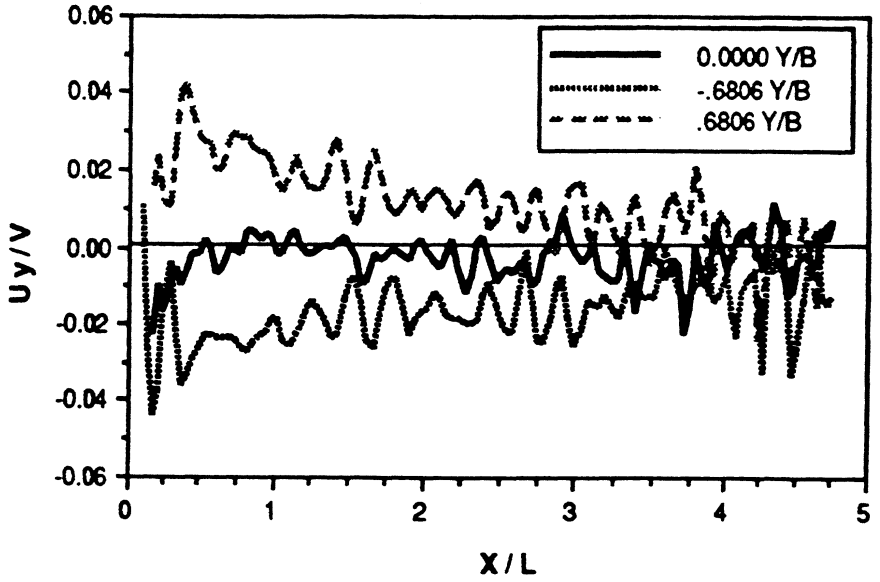

Figure 23. Cross-stream surface wake fractions as a function of distance starboard, for longitudinal cuts through Figure 21, light filtering (ω_x=0.35, L_x=5,ω_y=0.45,L_y=4).

unfiltered up to 3 ship lengths. This is displayed in Figures 22 and 23, and can be compared to the unfiltered plots in Figures 10 and 11. The noise at four to five ship lengths is dramatically reduced. Transverse plane cuts, shown in Figures 24 and 25, can be compared to their unfiltered plots in Figures 12 and 13.

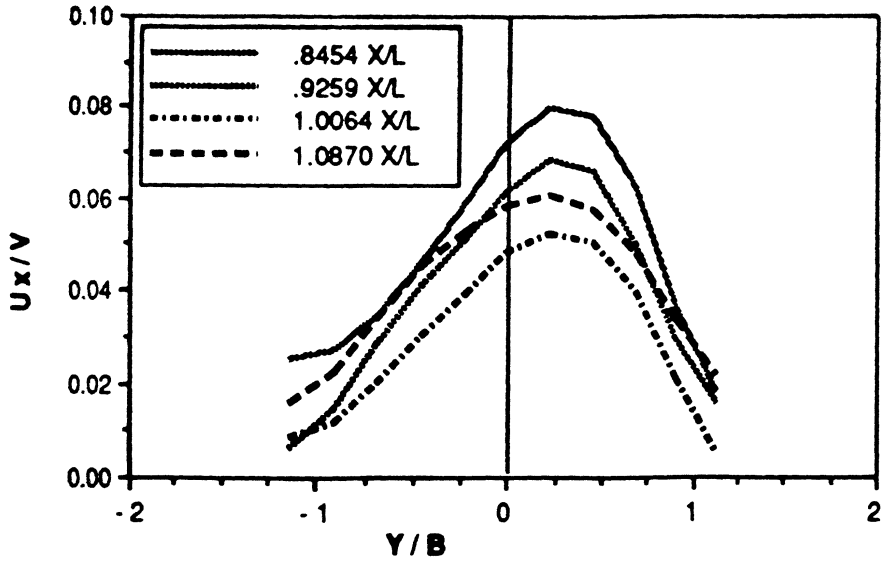

Figure 24. Downstream surface wake fractions as a function of distance starboard, for transverse cuts through Figure 20, light filtering (ω_x=0.35, L_x=5,ω_y=0.45,L_y=4).

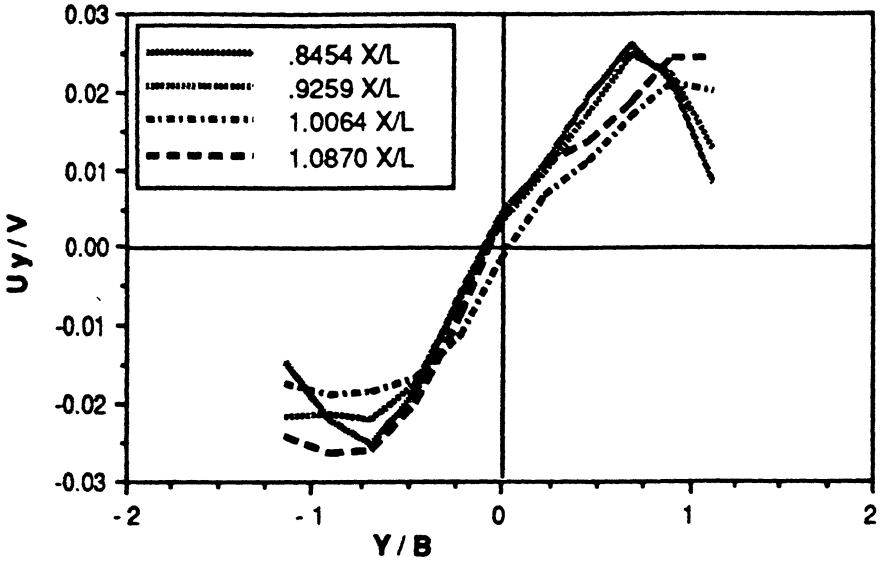

Figure 25. Cross-stream surface wake fractions as a function of distance starboard, for transverse cuts through Figure 21, light filtering (ω_x=0.35, L_x=5,ω_y=0.45,L_y=4).

3. Theoretical Comparison

For a theoretical comparison with the longitudinal plane cuts, calculations were made of Kelvin wave patterns in which the phase velocity equals the speed of the ship so that the characteristic transverse wave length λ, where

$$\lambda = 2 \cdot \pi \cdot V_p^2/g.$$

For this case, V_s = 6.772 feet per second (2.06 m/s) generating a wavelength of λ = 8.94 feet (2.72 m). Table II shows measurements from Figure 22 that indicate overall agreement with the Kelvin wave pattern. However, the waves decrease in wavelength with increasing distance downstream.

Table II. Transverse wavelengths measured from Figure 22.

Longitudinal Position - x/L	No. of wave orbital cycles	mean wavelength - ft (m)
0 to 1	2.5	9.94 (3.03)
1 to 2	3.0	8.28 (2.52)
2 to 3	3.5	7.10 (2.16)
overall	9.0	8.28 (2.52)

By modelling the Kelvin wave system as if it were generated by a pressure point located in front of the ship, good agreement is reached with the measured values and the theoretical positions where the first and second wall reflections should occur. For a towing tank with 22 foot (6.71 m) width, the model should have the first wall reflection cross the centerline at approximately 28 feet (8.53 m) and the second reflection about 90 feet (27.43 m) behind the model stern. Close examination of Figure 10 shows that the level of variance in the system seems to increase at those positions.

4. Hydrodynamic Insights

The asymmetry of W_x and W_y shows a greater axial velocity at the gree surface on the port side at the free surface (the near-field peak at x=10 feet (3.05 m) is at y = 0.5 feet (0.152 m)rather than at the centerline in Figure 20) and higher transverse velocities (W_y = +0.04 for starboard and -0.035 for port at x = 10 feet (3.05 m) in Figure 21) than the starboard side. One possible explaination for this assymetry is that the thrust wake from the shallower set port propeller provides a visible contribution to the surface flow field in the near wake.

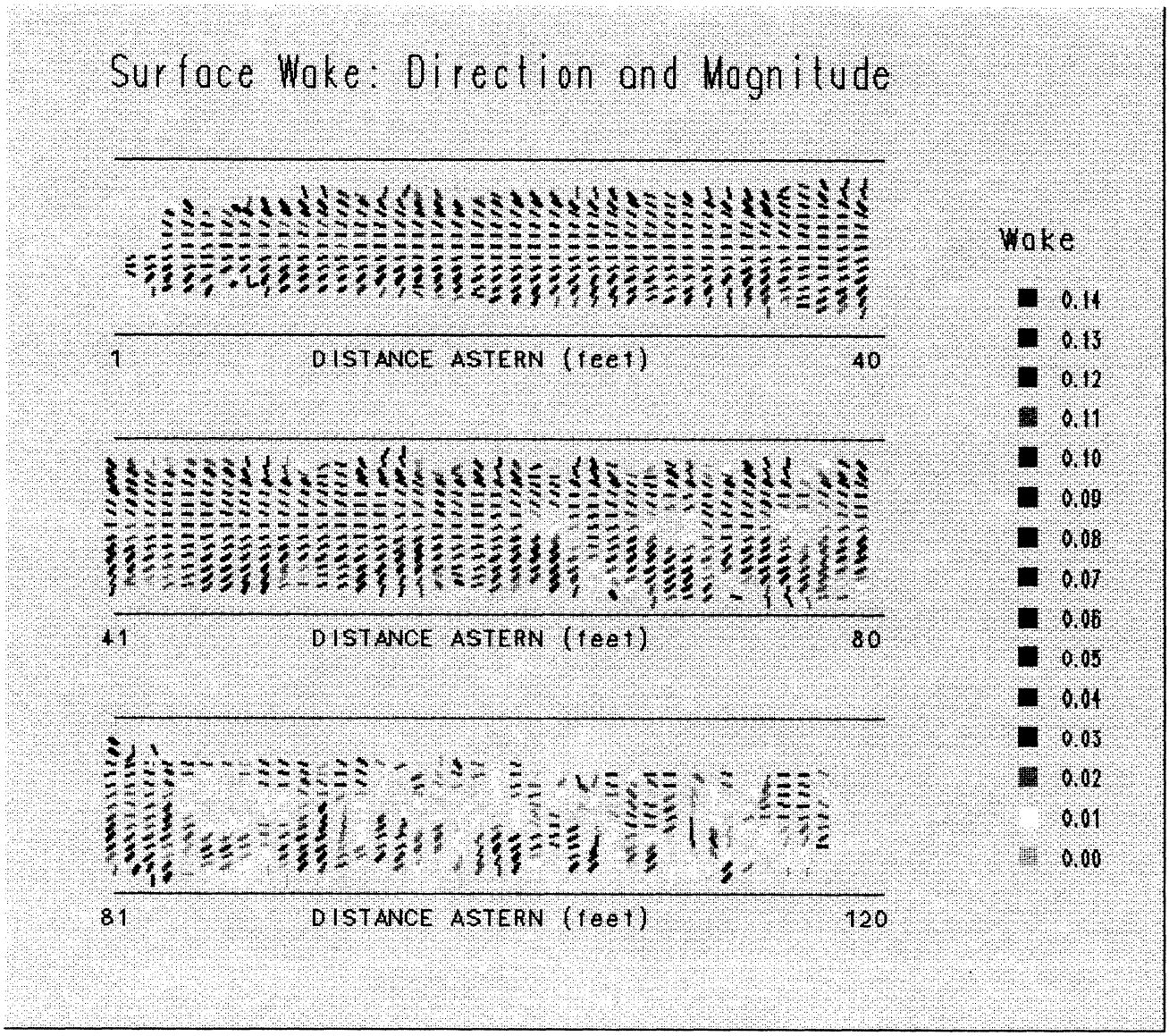

Figure 26. Vector diagram of lightly filtered surface wake fraction.

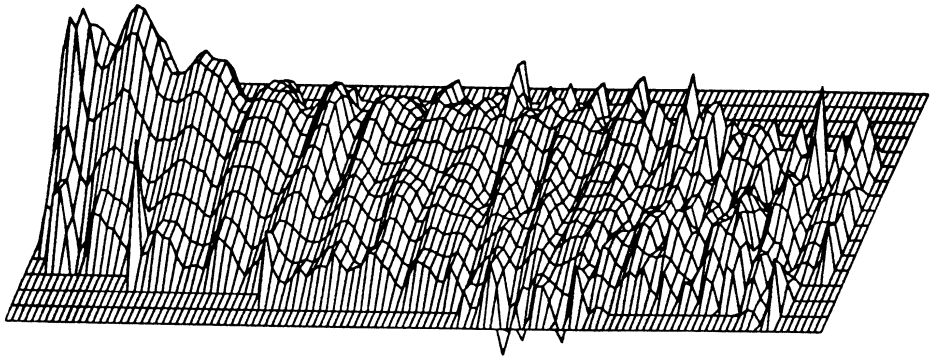

Figure 27. Two-dimensional plot of W_x.

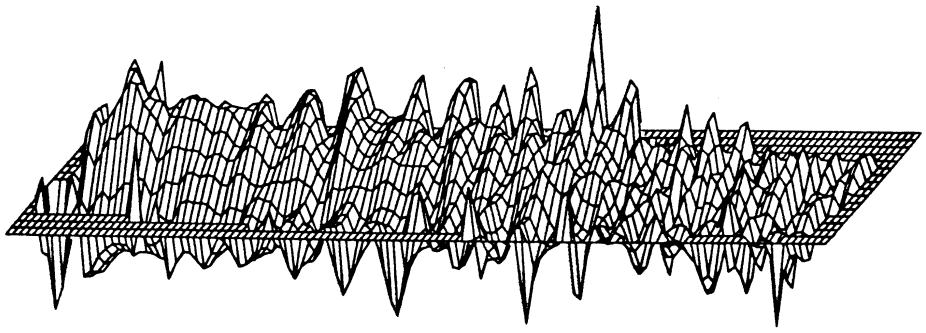

Figure 28. Two-dimensional plot of Wy.

Based on the appearance of wave orbital velocities in the dataset, measurements of transverse wavelength were made. The average transverse wave length was similar to a theoretical Kelvin pressure point wave system.

There is clear evidence of the wave reflections based on some increase in the noise of the system and comparison with presure point Kelvin wave generation, but this does not effect the oscillations of the wake patterns. Therefore, surface waves must have a small effect on surface wake, indeed, an assumption of linear independence seems justified.

By combining both x and y velocities on one graph, the effects of surface vorticity may be examined. Figure 26 is a unit vector diagram expressing velocity magnitude by color. Note that the velocities in both directions are very small far down stream but the vectors retain their unit length. A significant pattern can be seen in which every three or four bins has either purely longitudinal or purely transverse velocities along the edge. This gives evidence for sustained vorticity in the flow field. Figures 27 and 28 are two-dimensional plots of W_x and W_y respectively, which may help in visualizing the two velocity fields.

IV. CONCLUSIONS AND RECOMMENDATIONS

As a result of this investigation and subsequent detailed analysis of the composite data sets collected (approximately 30,000 velocity observations in the near wake region) the following conclusions are drawn.

With respect to the method of surface wake velocity measurement acquisition, this procedure was highly accurate. The level of error in digitizing target positions was less than one percent of the wake coverage. The use of 15 targets per run was sufficient to provide an even spread of velocity measurements throughout the wake field up to 90 feet (27.43 m) aft. The analysis could have extended farther if all records were digitized to their full 10 second extent.

Statistically, the number of individual velocities in each bin that exceeded three standard deviations from the bin mean velocity was about less than one percent of the total number of points digitized and accepted. This is consistent with minimum

standards for a normally distributed ensemble. Within each offset dataset, repeated runs of the same conditions are virtually identical. Runs with offset port or starboard positions were lightly filtered for excellent agreement. Filtering of the final data set proved to be an effective tool in data anlysis providing insight to the hydrodynamics influencing the surface wake velocities.

This method of data acquisition, reduction and analysis is sensitive enough to clearly show the orbital velocity influence of the Kelvin wave pattern, identification of the tank wall reflection, and a surface wake perturbation possibly due to the known hull asymmetry. In addition, it has been shown that the DARTS system could be used to detect and quantify vorticity if the the analysis is performed in a fixed inertial reference frame.

Finally, extraction of all of the information generated by this technique has not yet been exhausted, but requires additional detailed analysis. The quality of the data set, however, strongly suggests this analysis would produce extremely fruitful results.

Appendix A. Test run listing

		Model Test Data Runs for Model 1597				
Run No.	Speed (ft/s)	Dist. Aft (Lengths)	Transverse Position	Desired RPM (port/stbd)	Actual RPM (port/stbd)	Comments
1	6.772	0.00	center	483/483	not recorded	no timer
2	6.772	0.00	center	483/483	490/483	
3	6.772	0.00	center	483/483	485/482	
4	6.772	0.00	center	483/483	476/482	
5	6.772	0.00	center	483/483	491/483	
6	6.772	0.00	center	483/483	487/483	
7	6.772	0.00	center	483/483	482/483	
8	6.772	0.00	center	483/483	482/482	
9	6.772	0.50	center	483/483	482/483	no timer
10	6.772	0.50	center	483/483	*** / ***	Stbd shaft fell out of model
11	6.772	0.50	center	483/483	483/481	anomalous looking pattern
12	6.772	0.50	center	483/483	354/354	
13	6.772	0.50	center	483/483	483/484	
14	6.772	0.50	center	483/483	482/483	
15	6.772	0.50	center	483/483	483/483	
16	6.772	0.50	center	483/483	482/484	
17	6.772	0.50	center	483/483	485/484	
18	6.772	1.00	center	483/483	483/483	
19	6.772	1.00	center	483/483	483/483	
20	6.772	1.00	center	483/483	483/482	
21	6.772	1.00	center	483/483	482/484	
	***	***	***	***		zero run
22	6.772	1.00	center	483/483	482/484	
23	6.772	1.00	center	483/483	483/483	
24	6.772	1.60	center	483/483	483/483	
25	6.772	1.60	center	483/483	482/483	
26	6.772	1.60	center	483/483	484/483	
27	6.772	1.60	center	483/483	483/483	
28	6.772	1.60	center	483/483	483/483	darts didn't drop
29	6.772	0.07	center	dart dropper struck by stern wave:darts washed off		
30	6.772	0.07	center	dart dropper struck by stern wave:darts washed off		
warning new focus and scale due to lowered tank water level ****						
31	6.772	0.07	center	483/483	483/483	one port side dart fell off
	***	***	***	***		zero run
32	6.772	0.07	center	483/483	483/483	four port side darts fell off
33	6.772	0.07	center	483/483	483/483	
34	6.772	0.07	center	483/483	484/483	
35	6.772	0.07	center	483/483	483/483	
36	6.772	0.07	center	483/483	484/483	
37	6.772	0.07	center	483/483	355/483	port rpm too low
38	6.772	0.07	center	483/483	477/482	
39	6.772	0.21	center	483/483	482/483	
40	6.772	0.21	center	483/483	482/483	
41	6.772	0.21	center	483/483	483/482	

		Model Test Data Runs for Model 1597				
Run No.	Speed (ft/s)	Dist. Aft (Lengths)	Transverse Position	Desired RPM (port/stbd)	Actual RPM (port/stbd)	Comments
42	6.772	0.21	center	483/483	483/483	
43	6.772	0.21	center	483/483	486/484	
44	6.772	0.21	center	654/345	650/450	Begin trail shaft tests
45	6.772	0.21	center	654/345	653/435	
46	6.772	0.21	center	654/345	652/370	
	* * *	* * *	* * *	* * *		zero run
47	6.772	0.21	center	654/345	652/345	
48	6.772	0.21	center	654/345	652/345	
49	6.772	0.21	center	654/345	652/345	
50	6.772	0.21	center	654/345	652/345	
51	6.772	0.21	center	654/345	652/345	
52	6.772	0.07	center	654/345	652/345	
53	6.772	0.07	center	654/345	652/345	
54	6.772	0.07	center	654/345	652/345	
55	6.772	0.07	center	654/345	652/345	
56	6.772	0.07	center	654/345	652/345	
57	6.772	0.00	center	654/345	650/344	
58	6.772	0.00	center	654/345	651/345	
59	6.772	0.00	center	654/345	651/345	
60	6.772	0.00	center	654/345	651/345	
61	6.772	0.00	center	654/345	651/345	
62	6.772	0.50	center	654/345	650/345	
63	6.772	0.50	center	654/345	650/345	
64	6.772	0.50	center	654/345	650/345	
65	6.772	0.50	center	654/345	650/346	
	* * *	* * *	* * *	* * *		zero run
66	6.772	0.50	center	654/345	353/339	both props freewheeling
67	6.772	0.50	center	654/345	353/345	port prop freewheeling
68	6.772	0.50	center	654/345	654/343	
69	6.772	0.50	center	654/345	651/343	
70	6.772	1.00	center	654/345	651/344	
71	6.772	1.00	center	654/345	651/346	
72	6.772	1.00	center	654/345	651/345	
73	6.772	1.00	center	654/345	651/345	
74	6.772	1.00	center	654/345	651/345	
75	6.772	1.60	center	654/345	650/344	
76	6.772	1.60	center	654/345	650/344	
77	6.772	1.60	center	654/345	650/344	
78	6.772	1.60	center	654/345	655/345	
79	6.772	1.60	center	654/345	651/346	
80	6.772	1.60	14" port	654/345	650/345	
81	6.772	1.60	14" port	654/345	651/345	
82	6.772	1.60	14" port	654/345	651/345	
83	6.772	1.60	14" port	654/345	650/345	

		Model Test Data Runs for Model 1597				
Run No.	Speed (ft/s)	Dist. Aft (Lengths)	Transverse Position	Desired RPM (port/stbd)	Actual RPM (port/stbd)	Comments
	• • •	• • •	• • •	• • •		zero run
84	6.772	1.60	14" port	654/345	655/345	
85	6.772	1.60	14" port	654/345	654/345	
86	6.772	1.60	14" port	654/345	653/346	
87	6.772	1.60	14" port	654/345	652/345	
88	6.772	1.60	14" port	654/345	652/346	
89	6.772	1.00	14" port	654/345	651/345	
90	6.772	1.00	14" port	654/345	650/345	
91	6.772	1.00	14" port	654/345	649/345	
92	6.772	1.00	14" port	654/345	648/345	
93	6.772	1.00	14" port	654/345	648/345	
94	6.772	0.50	14" port	654/345	650/345	
95	6.772	0.50	14" port	654/345	649/345	
96	6.772	0.50	14" port	654/345	649/344	
97	6.772	0.50	14" port	654/345	649/344	
98	6.772	0.50	14" port	654/345	649/344	
99	6.772	0.21	14" port	654/345	647/345	
100	6.772	0.21	14" port	654/345	647/344	
101	6.772	0.21	14" port	654/345	648/344	
102	6.772	0.21	14" port	654/345	648/343	
103	6.772	0.21	14" port	654/345	648/344	
104	6.772	0.07	14" port	654/345	648/344	
	• • •	• • •	• • •	• • •		zero run
105	6.772	0.07	14" port	654/345	656/345	
106	6.772	0.07	14" port	654/345	651/345	
107	6.772	0.07	14" port	654/345	650/348	
108	6.772	0.07	14" port	654/345	650/346	
109	6.772	0.07	14" port	654/345	650/346	
110	6.772	0.00	14" port	654/345	650/346	
111	6.772	0.00	14" port	654/345	648/345	
112	6.772	0.00	14" port	654/345	648/345	
113	6.772	0.00	14" port	654/345	647/345	
114	6.772	0.00	14" port	654/345	647/345	
115	6.772	0.00	14" port	483/483	482/482	Standard shaft operation
116	6.772	0.00	14" port	483/483	483/482	
117	6.772	0.00	14" port	483/483	483/482	
118	6.772	0.00	14" port	483/483	484/483	
119	6.772	0.00	14" port	483/483	483/482	
120	6.772	0.07	14" port	483/483	484/484	
121	6.772	0.07	14" port	483/483	483/483	
122	6.772	0.07	14" port	483/483	482/482	
123	6.772	0.07	14" port	483/483	483/482	
124	6.772	0.07	14" port	483/483	482/483	
	• • •	• • •	• • •	• • •		zero run

		Model Test Data Runs for Model 1597				
Run No.	Speed (ft/s)	Dist. Aft (Lengths)	Transverse Position	Desired RPM (port/stbd)	Actual RPM (port/stbd)	Comments
166	6.772	0.21	14" stbd	483/483	483/483	
167	6.772	0.21	14" stbd	483/483	483/484	
168	6.772	0.21	14" stbd	483/483	483/483	
169	6.772	0.21	14" stbd	483/483	483/483	
170	6.772	0.07	14" stbd	483/483	484/483	
171	6.772	0.07	14" stbd	483/483	483/483	
172	6.772	0.07	14" stbd	483/483	483/483	
173	6.772	0.07	14" stbd	483/483	483/483	
174	6.772	0.07	14" stbd	483/483	483/483	
175	6.772	0.00	14" stbd	483/483	483/483	
176	6.772	0.00	14" stbd	483/483	483/483	
177	6.772	0.00	14" stbd	483/483	482/483	
178	6.772	0.00	14" stbd	483/483	483/483	
179	6.772	0.00	14" stbd	483/483	652/348	Trail shaft operation
	* * *	* * *	* * *	* * *		zero run
180	6.772	0.00	14" stbd	654/345	649/349	
181	6.772	0.00	14" stbd	654/345	650/345	
182	6.772	0.00	14" stbd	654/345	650/346	
183	6.772	0.00	14" stbd	654/345	649/347	
184	6.772	0.00	14" stbd	654/345	649/345	
185	6.800	0.07	14" stbd	654/345	650/346	
186	6.772	0.07	14" stbd	654/345	648/345	
187	6.772	0.07	14" stbd	654/345	645/347	
188	6.772	0.07	14" stbd	654/345	645/346	
189	6.772	0.07	14" stbd	654/345	648/345	
190	6.772	0.07	14" stbd	654/345	638/346	port rpm low
191	6.772	0.21	14" stbd	654/345	637/345	port rpm low
192	6.772	0.21	14" stbd	654/345	637/346	port rpm low
193	6.772	0.21	14" stbd	654/345	638/348	port rpm low
194	6.772	0.21	14" stbd	654/345	637/347	port rpm low
195	6.772	0.21	14" stbd	654/345	652/346	
196	6.772	0.50	14" stbd	654/345	648/346	
197	6.772	0.50	14" stbd	654/345	650/346	
198	6.772	0.50	14" stbd	654/345	650/346	
199	6.772	0.50	14" stbd	654/345	650/345	
200	6.772	0.50	14" stbd	654/345	650/345	
201	6.772	1.00	14" stbd	654/345	650/345	
202	6.772	1.00	14" stbd	654/345	648/345	
203	6.772	1.00	14" stbd	654/345	648/347	
204	6.772	1.00	14" stbd	654/345	648/345	
	* * *	* * *	* * *	* * *		zero run
205	6.772	1.00	14" stbd	654/345	660/347	
206	6.772	1.60	14" stbd	654/345	657/346	
207	6.772	1.60	14" stbd	654/345	655/346	

		Model Test Data Runs for Model 1597				
Run No.	Speed (ft/s)	Dist. Aft (Lengths)	Transverse Position	Desired RPM (port/stbd)	Actual RPM (port/stbd)	Comments
208	6.772	1.60	14" stbd	654/345	631/345	
209	6.772	1.60	14" stbd	654/345	632/345	
210	6.772	1.60	14" stbd	654/345	630/347	
211	6.772	1.60	14" stbd	654/345	not recorded	
212	6.772	1.60	center	no props	• • •	compare to 1987 data
213	6.772	1.60	center	no props	• • •	compare to 1987 data